Requirement for the L-type Ca^{2+} channel α_{1D} subunit in postnatal pancreatic β cell generation

Yoon Namkung,[1,2] Nataliya Skrypnyk,[1] Myung-Jin Jeong,[1] Taehoon Lee,[2] Myung-Shik Lee,[3] Hyung-Lae Kim,[4] Hemin Chin,[5] Pann-Ghill Suh,[2] Sung-Sook Kim,[6] and Hee-Sup Shin[1,2]

[1]National Creative Research Initiatives Center for Calcium and Learning, and
[2]Department of Life Science, Division of Molecular and Life Sciences, Pohang University of Science and Technology, Pohang, Korea
[3]Division of Endocrinology, Department of Medicine, Samsung Medical Center, Sungkyunkwan University College of Medicine, Seoul, Korea
[4]Department of Biochemistry, Medical College, Ewha Women's University, Seoul, Korea
[5]Genetics Research Branch, Division of Neuroscience and Basic Behavioral Science, NIH, Bethesda, Maryland, USA
[6]Department of Pathology, Ulsan University Hospital, Ulsan, Korea

Address correspondence to: Hee-Sup Shin, National CRI Center for Calcium and Learning, Korea Institute of Science and Technology, PO Box 131, Cheongryang, Seoul 130-650, Korea (South). Phone: 82-2-958-6931; Fax: 82-2-958-6919; E-mail: shin@kist.re.kr.

Received for publication May 18, 2001, and accepted in revised form August 13, 2001.

Pancreatic β cells are the source of insulin, which directly lowers blood glucose levels in the body. Our analyses of α_{1D} gene-knockout ($\alpha_{1D}^{-/-}$) mice show that the L-type calcium channel, α_{1D}, is required for proper β cell generation in the postnatal pancreas. Knockout mice were characteristically slightly smaller than their littermates and exhibited hypoinsulinemia and glucose intolerance. However, isolated $\alpha_{1D}^{-/-}$ islets persisted in glucose sensing and insulin secretion, with compensatory overexpression of another L-type channel gene, α_{1C}. Histologically, newborn $\alpha_{1D}^{-/-}$ mice had an equivalent number of islets to wild-type mice. In contrast, adult $\alpha_{1D}^{-/-}$ mice showed a decrease in the number and size of islets, compared with littermate wild-type mice due to a decrease in β cell generation. TUNEL staining showed that there was no increase in cell death in $\alpha_{1D}^{-/-}$ islets, and a 5-bromo-2′ deoxyuridine-labeling (BrdU-labeling) assay illustrated significant reduction in the proliferation rate of β cells in $\alpha_{1D}^{-/-}$ islets.

J. Clin. Invest. **108**:1015–1022 (2001). DOI:10.1172/JCI200113310.

Introduction

Voltage-dependent Ca^{2+} channels (VDCCs) provide a pathway for the entry of extracellular Ca^{2+} into the cytoplasm in a membrane voltage-dependent manner (1). VDCC is a heteromeric protein complex, composed of a pore-forming α_1 subunit and regularly associated β and disulfide-linked $\alpha_2\delta$ subunits (2). The L-type Ca^{2+} channel is defined by its pharmacological sensitivity to dihydropyridines, activation by relatively strong depolarization, and slow inactivation (3). Genes encoding the L-type channels are α_{1S}, α_{1C}, α_{1D}, and α_{1F} ($Ca_v1.1$-1.4) (4). Besides excitation-contraction coupling in muscle cells (5), L-type channels play critical roles in hormone or neurotransmitter release (6, 7), synaptic plasticity (8), and regulation of gene expression (9) especially in the nervous and neuroendocrine systems. Two different genes, α_{1C} and α_{1D}, encode neuronal L-type channels. The α_{1D} gene is expressed in various organs including brain, pancreas, heart, and cochlea (10–13).

Pancreatic β cells express the two isotypes of the L-type channel, α_{1C} and α_{1D} (11, 14). In the β cell, glucose metabolism causes an increase in ATP or the ATP/ADP ratio, which in turn closes K_{ATP} channels. This leads to membrane depolarization, opening of VDCC, influx of Ca^{2+}, and a rise in cytosolic free Ca^{2+} concentration ($[Ca^{2+}]_i$). The elevation of $[Ca^{2+}]_i$ directly triggers insulin exocytosis. L-type channels are known to play a physiological role in insulin secretion because L-type channel blockers inhibit the rise in intracellular calcium and insulin secretion in response to various insulin secretagogues (7). Analysis of mRNA encoding α_{1C} and α_{1D} demonstrated that the Ca^{2+}-conducting subunits of the L-type channel in pancreatic β cells mainly consist of the α_{1D} subunit (11, 14). On the basis of these considerations, we tried to elucidate the physiological role of α_{1D} in the pancreas by using α_{1D}-knockout ($\alpha_{1D}^{-/-}$) mice. Our results indicate that α_{1D} is required for the proper generation of β cells in the postnatal pancreas.

Methods

Generation of $\alpha_{1D}^{-/-}$ mice. α_{1D}-Deficient mice were generated using a conventional gene-targeting method (15). A murine α_{1D} genomic DNA clone containing the first two exons was isolated from a 129/svJae mouse genomic library. The region, spanning the 3′ end of the first exon to the 5′ β part of the second exon, was deleted and replaced with the IRES βgal expression cassette and *NEO* cassette. The *TK* (thymidine kinase with the *PGK* promoter) cassette, a negative selection marker, was inserted into the end of the 3′ homology region of the

targeting vector (Figure 1a), which was transfected into J1 embryonic stem (ES) cells. Chimeric mice, generated by injecting targeted ES cells into C57BL/6J blastocysts (16), were mated to C57BL/6J female mice to obtain germline transmissions of the mutation. Southern blotting was performed to genotype the progeny by using the genomic DNA fragment shown in Figure 1a as a probe (Figure 1b). The tail DNA was digested with *Bam*HI. Western blot analysis, using purified-monoclonal anti-α_{1D} antibody, confirmed the absence of α_{1D} proteins. Cerebral membrane proteins (30 μg) were separated on an 8–16% gradient SDS-PAGE gel (Invitrogen Corp., San Diego, California, USA). The mAb (α_{1D} 185-1) was raised against the α_{1D} peptide (RNKNSDKQRSA, corresponding to residues 2048-2058 of human α_{1D}) and purified as described previously (17).

Animals. The mice used had mixed genetic backgrounds of 129/svJae and C57BL/6J. Age- and sex-matched littermate animals were used as controls in all experiments. Animals were subjected to a 12-hour light/dark cycle, with free access to food and water. Animal care and handling was carried out according to the guidelines of the Pohang University of Science and Technology.

Blood glucose and insulin measurement. Intraperitoneal glucose tolerance tests were performed by injecting glucose (2 mg per g body weight), following an 18-hour overnight fast. Glucose levels in blood taken from the tails were determined using a One Touch Basic glucometer (Lifescan Canada Ltd., Burnaby, Canada). Blood was taken from the orbital sinus to measure serum insulin concentrations. Insulin tolerance tests were performed on randomly fed animals. Animals were injected with 0.75 IU/kg body weight human insulin (Humulin regular; Eli Lilly and Co., Indianapolis, Indiana, USA) into the peritoneal cavity. Blood glucose levels were measured immediately before and 15, 30, 45, and 60 minutes after the injection. Pancreatic insulin was extracted with acid ethanol for measuring extractable insulin. Insulin levels were determined using a rat insulin RIA kit (Linco Research Inc., St. Charles, Missouri, USA), with rat insulin as a standard.

Immunohistochemistry. Pancreas was carefully obtained from wild-type and $\alpha_{1D}^{-/-}$ mice. After weighing, pancreas was immediately fixed with 10% neutral buffered formalin, dehydrated in ethanol, and embedded in paraffin wax. Sections of paraffin-embedded pancreas of 5 μm thickness were incubated overnight with mouse anti-α_{1D} mAb (185-1; 1:200 dilution), anti-α_{1C} antibody (1:70 dilution; Alomone Labs, Jerusalem, Israel), guinea pig anti porcine-insulin (DAKO Corp., Glostrup, Denmark), glucagon (DAKO Corp.), pancreatic polypeptide (Zymed Inc., Camarillo, California, USA), or somatostatin (Zymed Inc.). They were further incubated with peroxidase-conjugated streptavidin complex (DAKO Corp.) for 30 minutes, followed by 3-ethyl carbazole (AEC) as a substrate chromogen (DAKO Corp.). Because the immunoreactivity of α_{1C} was too weak in wild-type pancreas, we used a signal amplification kit (CSA; DAKO Corp.) for α_{1C} staining in both wild-type and $\alpha_{1D}^{-/-}$ pancreas.

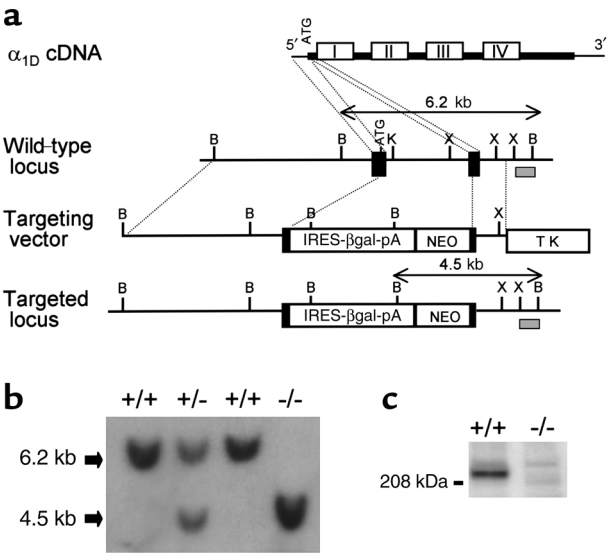

Figure 1
Targeted disruption of the calcium channel α_{1D} gene by homologous recombination. (**a**) A diagram of α_{1D} cDNA with the four transmembrane domains and structures of the wild-type locus, targeting vector, and targeted locus are shown. Restriction enzymes: B, *Bam*HI; X, *Xba*I; K, *Kpn*I. Solid boxes indicate exons. Hatched boxes underneath the wild-type and targeted locus signify the probe used for Southern blotting. IRES-βgal-pA was used for staining but, for unknown reasons, was not detectable in the mutant. *NEO*, neomycin-resistance gene with the *PGK* promoter. *TK*, thymidine kinase with the *PGK* promoter. (**b**) Genomic Southern blot on offspring from the heterozygote matings. The 6.2-kb band is the wild-type allele and the 4.5-kb band is the targeted allele. (**c**) Western blot of cerebral membrane fractions from wild-type and $\alpha_{1D}^{-/-}$ mice. M_r markers in kDa are indicated on the left. The mAb (α_{1D} 185-1) against the α_{1D} peptide (RNKNSDKQRSA, corresponding to residues 2048–2058 of human α_{1D}) specifically recognized a protein with a molecular weight of approximately 220 kDa from wild-type brain that was lacking in the mutant.

Electrophysiology. Pancreatic islets were isolated from 6- to 10-week-old mice by collagenase digestion, as described previously (18). For the patch clamp experiments, islets were dissociated in trypsin/EDTA (0.05% trypsin, 0.53% EDTA) for 5 minutes at 37°C. Dispersed islets were plated onto cover glasses and cultured for 2–4 days in RPMI 1640 supplemented with 10% FBS and penicillin-streptomycin. More than 80% of dispersed islet cells were insulin-positive β cells, as confirmed by immunocytochemistry, and they were usually bigger than insulin-negative cells. Consequently, only bigger cells were used for measuring the I_{Ba}. Whole-cell recordings were carried out as described previously (15), using 1–4 MΩ electrodes on islet cells. Series resistance ranged from 2 MΩ to 8 MΩ, and was compensated by 75–80%. Recordings were obtained with an Axopatch 200B amplifier (Axon Instruments Inc., Foster City, California, USA). The pClamp6 software (Axon Instruments, Inc.) was used to control all data acquisition and analysis. Currents were filtered 5 kHz, digitized at 100

μs per point, and leak-subtracted using a -P/4 procedure. Pipettes were filled with 130 mM CsCl, 4 mM $MgCl_2$, 5 mM TEA·Cl, 10 mM HEPES, 10 mM EGTA, 4 mM Na_2ATP, and 0.3 Na_2GTP 0.3 (pH 7.2), whereas the external solution comprised 130 mM NaCl, 4.8 mM KCl, 10 mM $BaCl_2$, 1.2 mM $MgCl_2$, 5 mM TEA·Cl, 10 mM HEPES, 2.8 mM glucose, and 0.001 mM tetrodotoxin (pH 7.2). Nifedipine (Sigma Chemical Co., St. Louis, Missouri, USA) was applied, using gravity from a linear array of glass capillaries.

Insulin secretion from pancreatic islets in vitro. Glucose-stimulated insulin secretion was measured by the method described previously (19). Islets isolated as described above were cultured for 48 hours in RPMI 1640 supplemented with 10% FBS and penicillin-streptomycin in a 60-mm Petri dish. Cultured islets, 100–200 μm in diameter, were selected after inspection under a microscope. Islets were preincubated in 5% CO_2 at 37°C for 1 hour in a 60-mm Petri dish containing HEPES-Krebs buffer composed of 118.4 mM NaCl, 4.7 mM KCl, 1.2 mM KH_2PO_4, 2.4 mM $CaCl_2$, 1.2 mM $MgSO_4$, 20 mM $NaHCO_3$, 3 mM glucose, and 10 mM HEPES (pH 7.4) supplemented with 0.2% BSA. After incubation, islets (5–10 per well) were transferred to a 24-well plate containing 0.3 ml buffer with various concentrations of glucose and were incubated under 5% CO_2 at 37°C for 30 minutes. After incubation, the supernatant was assayed for insulin content with an insulin RIA kit (Linco Research, Inc., St. Charles, Missouri, USA). To normalize insulin secretion per islet, insulin concentration was divided by the number of islets per well. Three or four independent experiments were carried out for each glucose concentration.

Measurement of pancreatic islet mass. To measure the number of islets in the whole pancreas, we counted the islets as described previously with some modifications in the method (20). The entire pancreas was dissected, weighed, and immersed in 10% buffered formalin. Those were embedded in paraffin and cut serially in 20-μm thickness. Every fifth section was stained with toluidine blue to count the islets. Photographs (200× or 400×) of pancreas sections (5 μm) were used to count the cell number per islet area. To avoid a bias, all the islets in each section were examined. Five female wild-type (85–148 islets per pancreas) and five female $\alpha_{1D}^{-/-}$ mice both at the age of 30 days old (56–84 islets per pancreas) were examined.

TUNEL staining. Apoptotic cells were identified in 5-μm paraffin-embedded sections of pancreas by in situ detection of DNA fragmentation, using the TUNEL method (ApopTag; Intergen Co., Purchase, New York, USA).

BrdU injections and immunohistochemistry. BrdU (Sigma Chemical Co.) was dissolved in 0.1 M phosphate buffer (pH 7.4). Female mice, at 14 and 30 days of age, were injected intraperitoneally with BrdU (50 mg per kg body weight) and sacrificed after 2 hours. Pancreas was dissected, weighed, and fixed with 10% formaldehyde. All staining was done on 5-μm paraffin-embedded sections of pancreas, pretreated with 3 N HCl for 30 minutes at 37°C to denature DNA. A mouse monoclonal anti-BrdU antibody (1:50; DAKO Corp.) was used. Immunoreactivities were visualized with biotin-streptavidin (LSAB kit; DAKO Corp.), using 3-ethyl carbazole (AEC) as a substrate chromogen. Double immunostaining for BrdU and insulin was performed, as described below. After staining for BrdU (see above), sections were blocked and incubated with guinea pig polyclonal anti-insulin antibody (1:100; DAKO Corp.). After overnight incubation at 4°C, sections were peroxidase labeled with Novostatin Super ABC kit, (Novocastra Laboratories Ltd., Newcastle, UK.) developed with DAB, and counterstained with hematoxylin. Cytosols of β cells stained dark violet, and BrdU-positive cells appeared with red nuclei. β Cells and BrdU-positive β cells were counted using an Olympus BX50 light microscope (Olympus Optical Co. Ltd., Tokyo, Japan) microscope and photographs (200× or 400×). A large number (2,000–5,000) of β cells were examined per animal.

Data analysis. A two-tailed, unpaired, Student's *t* test was used for statistical analysis. All values are expressed as mean ± SE.

Results

$\alpha_{1D}^{-/-}$ mice are deaf and smaller than their littermates. The $\alpha_{1D}^{+/-}$ heterozygotes showed no apparent abnormality and were fertile. Homozygotes ($\alpha_{1D}^{-/-}$) were obtained by mating heterozygotes (Figure 1b). Western blotting of

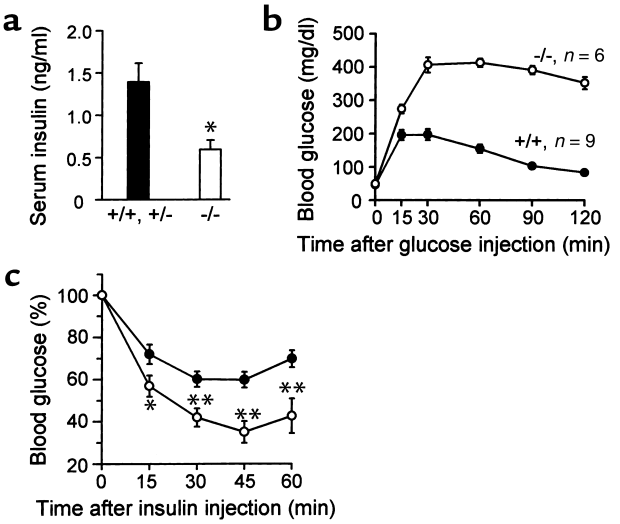

Figure 2
Serum insulin levels and glucose tolerance test. (**a**) Serum insulin concentrations in nonfasting 10-week-old $\alpha_{1D}^{-/-}$ mice (open bar, $n = 4$) and control littermates (filled bar, $n = 5$). *$P < 0.005$. (**b**) Glucose tolerance tests of 12- to 14-week-old female mice. Blood glucose was determined at indicated time points after intraperitoneal glucose injection (2 mg/g body weight). Open circles, $\alpha_{1D}^{-/-}$ mice ($n = 6$); filled circles, wild-type littermates ($n = 9$). (**c**) Insulin tolerance tests were performed on fed animals. Results are expressed as percentage of initial blood glucose concentration. Open circles, $\alpha_{1D}^{-/-}$ mice ($n = 7$); filled circles, control littermates ($n = 11$). *$P < 0.05$; **$P < 0.01$.

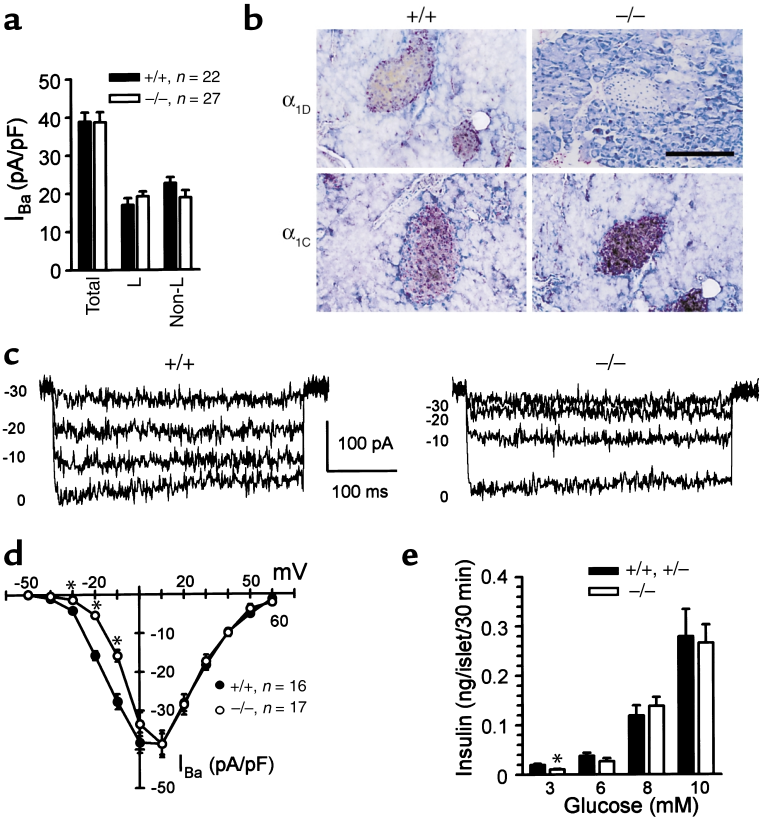

Figure 3
Ca^{2+} channel activities in pancreatic islet cells. (**a**) The current density histogram of peak I_{Ba} in wild-type (filled bars, n = 22) and $\alpha_{1D}^{-/-}$ (open bars, n = 27) islets. Total refers to total current density; L represents L-current density; Non-L is the remaining current density. I_{Ba} was activated by depolarizations from –80 mV to 0 or 10 mV every 10 seconds. (**b**) Immunostaining of L-type calcium channel subtypes in pancreatic islets. Primary antibodies used are indicated on the left side of the panel. Four independent experiments were performed from three animals per genotype. Bar, 100 μm. (**c**) Representative current records of I_{Ba} by whole cell patch clamp in wild-type and $\alpha_{1D}^{-/-}$ pancreatic islet cells. Depolarizations from –80 mV to levels ranging from –30 to 0 mV in 10-mV increments for 400 microseconds every 10 seconds. (**d**) Voltage dependence of Ca^{2+} channel currents in wild-type (filled circles, n = 16) and $\alpha_{1D}^{-/-}$ (open circles, n = 17) β cells. *P < 0.001. The peak I_{Ba} current was normalized to cell capacitance. Average cell capacitance was 4.35 ± 0.32 pF for $\alpha_{1D}^{-/-}$ islet cells and 4.16 ± 0.17 pF for wild-type islet cells. (**e**) Stimulation of insulin release from cultured islets by glucose stimulation. Islets of similar sizes were selected from the $\alpha_{1D}^{-/-}$ (open bars) and the control mice ($\alpha_{1D}^{+/+}$ and $\alpha_{1D}^{+/-}$, filled bars). Five to seven animals were used per genotype. The number of measurements (n) for each concentration for each genotype ranged from 4 to 25. *P < 0.05.

cerebral membrane proteins (Figure 1c) and immunostaining of pancreas sections (see Figure 3b) confirmed the lack of α_{1D} protein in knockout mice. Homozygous $\alpha_{1D}^{-/-}$ mice appeared healthy, but smaller (80% of normal body weight) than the littermate controls. The lack of motor reflex in $\alpha_{1D}^{-/-}$ mice in response to an auditory stimulus (Preyer reflex) and the significantly elevated auditory brainstem response (ABR) threshold for a broadband click (data not shown) confirmed that $\alpha_{1D}^{-/-}$ mice were deaf, consistent with the phenotype of α_{1D} knockout mice reported by Platzer et al. (13).

$\alpha_{1D}^{-/-}$ mice are hypoinsulinemic and glucose intolerant. Given that α_{1D} is the dominant L-type channel protein in pancreatic β cells (11, 14), and inhibitors of L-type channels block most of the glucose-stimulated and depolarization-evoked insulin release (7), we investigated blood glucose homeostasis in the mutants. In nonfasting states, the serum insulin levels in adult $\alpha_{1D}^{-/-}$ mice were lower than those observed in littermate control mice (Figure 2a), although blood glucose levels did not differ significantly between the wild-type and mutant mice (154.1 ± 8.9 mg/dl, n = 7 males, wild-type; 159.1 ± 17.7 mg/dl, n = 8 males, $\alpha_{1D}^{-/-}$, P = 0.81). Glucose tolerance tests were performed to verify the pancreatic dysfunction in $\alpha_{1D}^{-/-}$ mice. As shown in Figure 2b, at 12–14 weeks of age, $\alpha_{1D}^{-/-}$ mice remained hyperglycemic 2 hours after intraperitoneal injection of glucose, whereas in the wild-type mice, blood glucose levels returned to the baseline. The level of serum insulin increased twofold in wild-type mice 30 minutes after glucose injection (after overnight fasting, i.e., before glucose injection, 0.24 ± 0.06 ng/ml, n = 6; 30 minutes after glucose injection, 0.49 ± 0.07 ng/ml, n = 6). We could not quantify the serum insulin in mutant mice, because for the majority of the mutants, the serum insulin levels after overnight fasting were less than 0.1 ng/ml (n = 7), which was the lowest limit of the insulin measuring kit used. Serum insulin levels in $\alpha_{1D}^{-/-}$ mice, measured 30 minutes after glucose injection, were still below 0.1 ng/ml (n = 5). These data suggest that glucose intolerance in the $\alpha_{1D}^{-/-}$ mice might be caused by the insulin deficiency. However, $\alpha_{1D}^{-/-}$ mice exhibited normoglycemia in fed states compared with age-matched littermates and did not develop diabetes over the 1-year observation period. Because enhanced insulin sensitivity might account for these results in $\alpha_{1D}^{-/-}$ mice, we injected insulin and examined changes in blood glucose levels. Indeed, the glucose-lowering effect of insulin was significantly enhanced in $\alpha_{1D}^{-/-}$ mice, compared with wild-type mice (Figure 3c).

Compensatory overexpression of α_{1C} in $\alpha_{1D}^{-/-}$ pancreatic β cells. Given that calcium entry through L-type calcium channels is crucial for insulin secretion in β cells (7), we examined the effects of the loss of the α_{1D} channel on calcium currents and insulin secretion in response to glucose stimulation in $\alpha_{1D}^{-/-}$ pancreatic β cells. Ca^{2+} currents, supported by 10 mM Ba^{2+} as a charge carrier, were activated by step depolarizations from a holding potential of –80 mV. Unexpectedly, mutant cells did not show a decrease in either total current density (Figure 3a) or

Figure 4
Islet morphology. (**a**) Upper panel: insulin- and glucagon-positive cells, respectively in wild-type and mutant mice. Bars, 100 μm. Lower panel: lower magnification (×40) of pancreatic islets of wild-type and $\alpha_{1D}^{-/-}$ mice. Immunostaining with anti-insulin antibody shows sparse distribution and lack of larger islets in the $\alpha_{1D}^{-/-}$ pancreas. (**b**) Decreased number of islets in $\alpha_{1D}^{-/-}$ mice, compared with that in littermate controls. Summed islet numbers obtained from examining every fifth section of 20-μm thickness from a whole pancreas. Filled bars, littermate control mice (wild-type for P0, P14, and P30 and heterozygote for 7 months); open bars, $\alpha_{1D}^{-/-}$ mice. The number of animals examined is indicated at the bottom of each bar. $^*P < 0.05$. $^{**}P < 0.001$. (**c**) Morphometric analysis of islet area in pancreas from wild-type (filled bars, $n = 5$) and $\alpha_{1D}^{-/-}$ (open bars, $n = 5$) female mice at P30. Distribution of islet areas less than 100 cells, 100–150 cells, or more than 150 cells is shown as a percentage of islets measured. The proportion of larger islets (more than 150 cells in a cross-section) was significantly reduced in the $\alpha_{1D}^{-/-}$ pancreas. $^*P < 0.05$. (**d**) Percentage of β cells in individual islets at P30. Filled bar, wild-type islets ($n = 58$ islets from five mice); open bar, $\alpha_{1D}^{-/-}$ islets ($n = 79$ islets from five mice). $^*P < 0.001$.

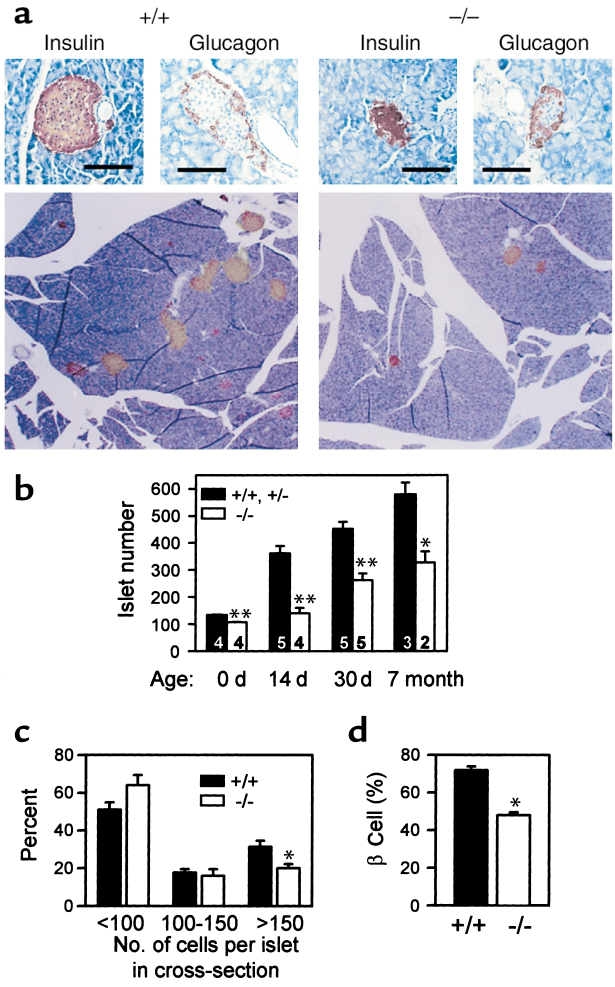

L-type current density, as confirmed by current analyses in the presence of 10 μM nifedipine (Figure 3a). These results suggest the possibility of a compensatory increase in the other L-type channel, namely α_{1C}. Immunostaining with anti-α_{1C} antibody confirmed that α_{1C} was indeed overexpressed in mutant pancreatic islets, compared with wild-type mice (Figure 3b). Significantly, a closer examination of electrophysiological data revealed that a current-voltage plot of the mutant cells was shifted by about 10 mV toward more positive potentials at the lower voltage range (Figure 3d). Therefore, the current density at –10 mV and –20 mV were reduced by approximately 50% and approximately 70% in mutant β cells, respectively (Figure 3d). However, at potentials of 10 mV or above, the curves looked virtually identical between mutant and wild-type. These results effectively demonstrate the loss of α_{1D} channels and subsequent compensation by α_{1C} in the mutant, as α_{1D} channels have a lower activation threshold than α_{1C} (10, 13). Because β cell action potentials in response to glucose stimulation rarely exceed –10 mV (21, 22), the decreased channel activity below the membrane potential of –10 mV in mutant β cells may affect the secretion of insulin. To examine the consequences of the altered channel profile on the insulin secretory function of islet β cells, we measured insulin secretion from isolated islets in culture in response to ambient glucose, using the batch incubation method. Mutant islets secreted less insulin than control islets at 3 mM ambient glucose (0.019 ± 0.003 ng/30min/islet for control; 0.011 ± 0.002 ng/30min/islet for mutant; $P = 0.03$), although no statistically significant difference was observed at glucose concentrations of 6 mM or higher (Figure 3e). These results suggest that the glucose-sensing and subsequent insulin secretion machinery might be largely preserved in isolated α_{1D}-deficient β cells.

Reduction of β cell mass in $\alpha_{1D}^{-/-}$ pancreas. Another possible mechanism underlying the hypoinsulinemia and glucose intolerance in $\alpha_{1D}^{-/-}$ mice could be a reduction of

Figure 5
β Cell proliferation rate. (**a**) Anti-BrdU and anti-insulin double immunostaining of pancreatic islets. The β cells have dark violet cytosols, and BrdU-positive cells appear with red nuclei. Representative islets each from the wild-type (left) and the $\alpha_{1D}^{-/-}$ mice (right) at P14 were shown. Bar, 50 μm. (**b**) Reduced β cell proliferation rate in the $\alpha_{1D}^{-/-}$ islets. The percentage of BrdU-positive β cells among β cells was obtained from each mouse, and the average value was calculated for each genotype. Filled bars, wild-type ($n = 5$ mice for P14 and P30); open bars, $\alpha_{1D}^{-/-}$ ($n = 2$ mice for P14 and $n = 5$ mice for P30). $^*P = 0.05$; $^{**}P < 0.005$.

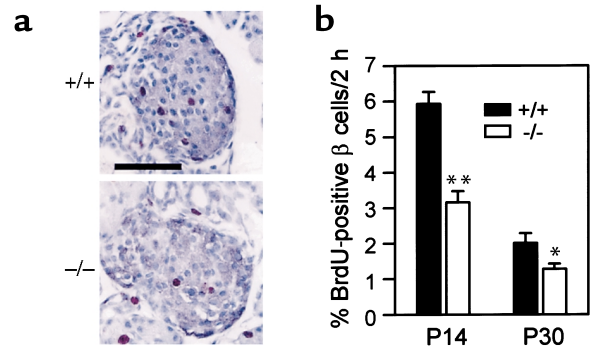

total β cell mass. We examined islet morphology in the mutant pancreas. Pancreatic islets of $\alpha_{1D}^{-/-}$ mice were well organized with the insulin-producing β cells forming a central core surrounded by a discontinuous mantle of non β cells (Figure 4a). A simple scanning of the histological slides under a microscope, however, revealed a marked decrease in islet numbers and a scarcity of larger islets in the mutant pancreas, compared with control (Figure 4a). At the day of birth (P0), mutant mice showed smaller body weight and a slightly smaller number of islets (Figure 4b), although the relative islet number (normalized as their body weight) was equivalent to that in littermate wild-type mice (88.1 ± 3.9 per body weight in wild-type mice, and 81.8 ± 3.1 per body weight in $\alpha_{1D}^{-/-}$ mice at birth [n = 4]; P = 0.24). However, at postnatal day 14 (P14), the islet number was approximately 60% less than that of wild-type littermates, and by P30, we observed approximately 40% fewer islets than in wild-type littermates (Figure 4b). The relative islet number was also significantly reduced in $\alpha_{1D}^{-/-}$ pancreas by approximately 40% at P14 (n = 4, P < 0.05) and approximately 30% at P30 (n = 5, P < 0.05). But the pancreas weight (measured as percent body weight) did not differ between the $\alpha_{1D}^{-/-}$ mice and littermate controls (0.25 ± 0.01% for wild-type mice versus 0.28 ± 0.01% for $\alpha_{1D}^{-/-}$ mice at P14, P = 0.15; 1.15 ± 0.05% versus 1.25 ± 0.03% at P30, P = 0.15d). Distribution of islet size (shown in Figure 4 by cell numbers in the cross-section), represented as a percentage of islets measured, revealed a significant reduction in the number of larger islets in the mutant pancreas (Figure 4c). The proportion of β cells in individual islets was significantly reduced, from approximately 72% in wild-type islets to approximately 48% in mutant islets (Figure 4d). Moreover, the percentage of α cells was relatively increased in mutant islets (data not shown), indicating that reduction of islet mass was mostly caused by a decrease in β cell mass. Somatostatin- and pancreatic polypeptide–positive cells were well preserved in the mutant islets (data not shown). Our data collectively demonstrate that postnatal β cell expansion is impaired in $\alpha_{1D}^{-/-}$ mice. The reduction in β cell mass may, in turn, lead to hypoinsulinemia and glucose intolerance in $\alpha_{1D}^{-/-}$ mice.

Decreased β cell proliferation in the $\alpha_{1D}^{-/-}$ mice. To determine whether the decrease in β cell mass was due to a defect in β cell genesis or in survival, we first examined the degree of cell death in islets at P14 and P30, using the TUNEL assay. Previously, it was reported that the frequency of apoptotic β cells is higher throughout the neonatal period than in the adult rat, peaking at 13–17 days after birth (23). We found no increase in the cell death in mutant islets either at P14 or P30. At P14, the percentage of apoptotic cells was 5.73 ± 0.01% in wild-type islets (n = 2 mice) and 5.42 ± 0.17% in mutant islets (n = 2 mice). At P30, there were only six apoptotic cells over 49 islets in the wild-type and four cells over 41 islets in the mutant pancreas, respectively. This indicates that the decrease in β cell mass in the mutant was not due to an increase in cell death but rather due to a decrease in the proliferation and/or differentiation of β cells. Pancreatic β cell growth can be mediated by neogenesis or differentiation from ductal precursor cells, and replication of differentiated β cells (24, 25). β Cell neogenesis and replication normally proceeds in mice up to around 3 weeks of age (26, 27). After weaning, a low level of replication is maintained (24). As shown in Figure 4b, during the first 2 weeks after birth, increase in islet number was severely impaired in the mutant pancreas. We examined β cell proliferation at P14, by incorporation and immunohistochemical detection of bromodeoxyuridine (BrdU) in the DNA of dividing cells. After 2-hour BrdU labeling, the number of BrdU and insulin double-positive cells per total insulin-positive cells significantly decreased in mutant islets to 53% of that in wild-type at P14, and the difference persisted at P30 (Figure 5b). In conclusion, the β cell proliferation rate is decreased in the mutant islets, and this may partly contribute to the decrease in β cell mass in $\alpha_{1D}^{-/-}$ mice.

Discussion

In the present study, we show a marked reduction in total islet mass in $\alpha_{1D}^{-/-}$ mice, due to impairment of postnatal β cell generation. The actual β cell mass in $\alpha_{1D}^{-/-}$ mice at P30 is approximately 24–30% of that of wild-type mice, as the total islet number in mutant is approximately 60% of that in wild-type (Figure 4b), and the number of β cells in individual islets is approximately 40–50% of that in wild-type (Figure 4d).

We observed an overexpression of α_{1C} in islets of $\alpha_{1D}^{-/-}$ mice both in adult (Figure 3b) and at P14 (data not shown). The maximal current density was restored in the mutant β cells, although the calcium current density at –10 mV to –30 mV was reduced by 50–70% in mutant β cells (Figure 3d). In spite of the compensatory overexpression of α_{1C} in mutant β cells and the normal maximal current density, proliferation rate was reduced. These results may suggest two possible roles of α_{1D} in β cell proliferation. First, calcium entry through α_{1D} channels at the membrane potentials of below –10 mV may play a role in β cell proliferation. Second, α_{1D} protein itself may function as one of the components in the mitogenic signaling pathway. These two possibilities do not necessary exclude each other. For the first time, to our knowledge, this study demonstrates that the L-type channel α_{1D} is one of the major requirements for proper β cell generation. In addition, these results clearly demonstrate distinct functions of the L-type channel isotypes in the pancreas.

The β cell mass reduction in $\alpha_{1D}^{-/-}$ mice is an unexpected and novel finding, as there have been no reports to show that L-type channels contribute to postnatal β cell generation. With hindsight, however, earlier observations are consistent with the possible involvement of L-type channels in the production of β cells. In pancreatic β cells, glucose uptake leads to an increase in intracellular ATP/ADP ratio and a closure of K_{ATP} channels. This results in membrane depolarization, opening of VDCC, calcium influx, and finally activation of the insulin secretory machinery. It is known

that glucose itself induces β cell mitosis in vivo or in vitro (28). Glibenclamide, a hypoglycemic drug that inhibits K_{ATP} channels, affects the replication rate and mass of β cells in young mice (29). Moreover, glucagon-like peptide-1 (GLP-1), a regulator of postnatal β cell growth and differentiation, increases levels of β cell cAMP and glucose-stimulated Ca^{2+} influx (30). Recent studies have shown that islet size and function may be determined by the extent of activin receptor-mediated TGF-β signaling (31). Pancreatic expression of a dominant negative type II activin receptor (dn-ActR) in transgenic mice results in islet hypoplasia (32, 33), and *ActRIIA*$^{+/-}$*B*$^{+/-}$ mice show hypoplastic pancreatic islets, hypoinsulinemia, and impaired glucose tolerance (34). Interestingly, activin causes Ca^{2+} influx through membrane depolarization by inhibiting the activity of the K_{ATP} channel and directly modulates VDCCs in β cells (35). However, until now, there have been no reports that L-type channels are involved in the β cell growth-promoting activity of GLP-1 and activin.

Recent studies have demonstrated that a number of transcription factors are necessary in the proper development of the pancreas (31). Genetic studies have outlined the hierarchy of transcription factors involved in β cell development. For example, the homeodomain factor, *IPF1/PDX1*, has been proposed to regulate the expression of a variety of different pancreatic endocrine genes including insulin, somatostatin, glucokinase, and glucose transporter 2 (Glut2). Recently, Hart et al. reported that attenuation of FGF signaling in mouse β cells leads to impairment of postnatal β cell expansion (36) and the expression of glucose transporter 2 (Glut2) in these mice. Moreover, the expression of FGF receptors was impaired in *IPF1/PDX1* inactivated β cells, and it was claimed that the *IPF1/PDX1* acts upstream of FGF receptor (FGFR) signaling. It would therefore be worthwhile to examine the levels of α_{1D} gene expression in these mice and the transcriptional regulation of α_{1D} gene in β cell development.

Contrary to our results, Platzer et al. (13) reported recently that α_{1D}-deficient mice showed no growth retardation or glucose intolerance. There are a number of possible explanations for this discrepancy. First, the difference in the genetic background of the embryonic stem (ES) cell line used for generating knockout mouse might have caused different phenotypes: AB2.2 originating from the 129/SvEv substrain was used in their work, whereas J1 originating from the 129/SvJae substrain was used in our work (37). The genetic heterogeneity among 129 substrains is well documented (37, 38). The phenotypes resulting from the disruption of genes in insulin production and insulin signaling pathways are critically dependent on the genetic background of the mouse used (39–41). Second, we used a different targeting strategy to the other group. For example, we deleted the locus spanning the 3′ end of the first exon to the 5′ part of the second exon that included an intron in between, whereas they inserted neocassette into the second exon. Further molecular analysis of each mutant with regard to the status of the α_{1D} locus, such as aberrantly spliced products, may provide an answer.

Despite the reduction of β cell proportion in individual $\alpha_{1D}^{-/-}$ islets (Figure 4d) and the decrease in Ca^{2+} channel activity at the lower range of membrane potentials in mutant β cells (Figure 3d), there is no decrease in insulin secretion in response to glucose stimulation except at the basal glucose concentration in $\alpha_{1D}^{-/-}$ islets (Figure 3e). This discrepancy implies that insulin secretion per β cell may be enhanced in mutant islets. In fact, analysis of insulin content in individual islets revealed that mutant islets contained more insulin than did similar size of wild-type islets (41.0 ± 2.4 ng/islet in mutant islets, n = 63 islets from three mice; 27.8 ± 2.2 ng/islet in wild-type islets, n = 66 islets from three wild type mice, $P < 0.001$). Considering the decreased proportion of β cells in mutant islets (Figure 4d), insulin content per β cell increased twice in mutant islets. However, it is unlikely that there is an increase in individual β cell volume (hypertrophy) in $\alpha_{1D}^{-/-}$ islets, because no significant difference was observed in cell capacitance (pF) between wild-type and $\alpha_{1D}^{-/-}$ cells (Figure 3b, legend). This increase in insulin content per islet accounts for the increase in insulin secretion from mutant islets. The average total insulin content in the pancreas (μg/g pancreas) in 6- to 7-week-old $\alpha_{1D}^{-/-}$ mice was approximately 39% that of control mice, which indicates that total β cell number might be approximately 20%, compared with wild-type mice.

It will be interesting to see whether there is any difference in the change of membrane potential in response to glucose between the wild-type and the mutant β cells. Glucose-induced membrane depolarization is the intervening step from glucose-sensing to insulin secretion (42). In addition, inward Ca^{2+} currents through VDCCs participate in the generation of action potentials in β cells (42). There is, however, a great deal of heterogeneity among β cells (22, 43), and the electrical activity of β cells induced by glucose is dependent on the cell configuration, such as in single cell, a cluster, or an intact islet (21, 22, 43). Therefore, this issue could be addressed by population studies using perforated patch-clamp recordings of β cells in intact pancreatic islets of wild-type and mutant mice (21).

The α_{1D}-deficient mice showed hypoinsulinemia and severely impaired glucose tolerance, which were caused mainly by the reduction of total β cell mass. Increases in insulin content in individual β cells and enhanced insulin sensitivity of peripheral tissues may offer explanations for the lack of overt diabetes in $\alpha_{1D}^{-/-}$ mice. Similar phenotypes such as impaired glucose tolerance and enhanced insulin sensitivity are observed in the offspring of insulin-sensitive type 2 diabetes patients (44, 45).

Human type 2 diabetes is strongly associated with genetic and familial backgrounds (46, 47). Although insulin resistance is an important pathological sign in the early stages of type 2 diabetes, a failure in adequate β cell mass increase leads to progression to a diabetic state (48). For example, humans with type 2 diabetes

have reduced β cell mass, compared with weight-matched nondiabetic subjects (48). Although mice lacking α_{1D} did not develop overt diabetes in the 12-month observation period, they might be more prone to diabetogenic conditions such as high-fat diet, stress, or mild insulin resistance, owing to reduced β cell mass. The possibility of using $\alpha_{1D}^{-/-}$ mice as a model for type 2 diabetes remains to be examined.

Acknowledgments

The authors thank M.P. Kong for animal care, K. Jun for primary library screening, J. Jeong for technical help, and J.W. Yoon for critical evaluation of the manuscript. This work was supported in part by a Creative Research Initiative program grant from the Ministry of Science and Technology, Korea, and a medical science grant from the Ministry of Health and Welfare, Korea.

1. Tsien, R.W., and Wheeler, D.B. 1999. Voltage-gated calcium channels. In *Calcium as a cellular regulator*. E. Carafoli and C.B. Klee, editors. Oxford University Press. New York, New York, USA. 171–199.
2. Reuter, H. 1996. Diversity and function of presynaptic calcium channels in the brain. *Curr. Opin. Neurobiol.* **6**:331–337.
3. Nowycky, M.C., Fox, A.P., and Tsien, R.W. 1985. Three types of neuronal calcium channel with different calcium agonist sensitivity. *Nature.* **316**:440–443.
4. Ertel, E.A., et al. 2000. Nomenclature of voltage-gated calcium channels. *Neuron.* **25**:533–535.
5. Mikami, A., et al. 1989. Primary structure and functional expression of the cardiac dihydropyridine-sensitive calcium channel. *Nature.* **340**:230–233.
6. Simmons, M.L., Terman, G.W., Gibbs, S.M., and Chavkin, C. 1995. L-type calcium channels mediate dynorphin neuropeptide release from dendrites but not axons of hippocampal granule cells. *Neuron.* **14**:1265–1272.
7. Devis, G., Somers, G., Van Obberghen, E., and Malaisse, W.J. 1975. Calcium antagonists and islet function. I. Inhibition of insulin release by verapamil. *Diabetes.* **24**:247–251.
8. Murphy, T.H., Worley, P.F., and Baraban, J.M. 1991. L-type voltage-sensitive calcium channels mediate synaptic activation of immediate early genes. *Neuron.* **7**:625–635.
9. Deisseroth, K., Heist, E.K., and Tsien, R.W. 1998. Translocation of calmodulin to the nucleus supports CREB phosphorylation in hippocampal neurons. *Nature.* **392**:198–202.
10. Williams, M.E., et al. 1992. Structure and functional expression of α_1, α_2, and β subunits of a novel human neuronal calcium channel subtype. *Neuron.* **8**:71–84.
11. Seino, S., et al. 1992. Cloning of the α_1 subunit of a voltage-dependent calcium channel expressed in pancreatic β cells. *Proc. Natl. Acad. Sci. USA.* **89**:584–588.
12. Kollmar, R., Montgomery, L.G., Fak, J., Henry, L.J., and Hudspeth, A.J. 1997. Predominance of the α_{1D} subunit in L-type voltage-gated Ca^{2+} channels of hair cells in the chicken's cochlea. *Proc. Natl. Acad. Sci. USA.* **94**:14883–14888.
13. Platzer, J., et al. 2000. Congenital deafness and sinoatrial node dysfunction in mice lacking class D L-type Ca^{2+} channels. *Cell.* **102**:89–97.
14. Iwashima, Y., et al. 1993. Expression of calcium channel mRNAs in rat pancreatic islets and downregulation after glucose infusion. *Diabetes.* **42**:948–955.
15. Namkung, Y., et al. 1998. Targeted disruption of the Ca^{2+} channel β_3 subunit reduces N- and L- type Ca^{2+} channel activity and alters the voltage-dependent activation of P/Q-type Ca^{2+} channels in neurons. *Proc. Natl. Acad. Sci. USA.* **95**:12010–12015.
16. Cho, C.H., Kim, S.S., Jeong, M.J., Lee, C.O., and Shin, H.S. 2000. The Na^+-Ca^{2+} exchanger is essential for embryonic heart development in mice. *Mol. Cells.* **10**:712–722.
17. Suh, P.G., Ryu, S.H., Choi, W.C., Lee, K.Y., and Rhee, S.G. 1988. Monoclonal antibodies to three phospholipase C isozymes from bovine brain. *J. Biol. Chem.* **263**:14497–14504.
18. Wollheim, C.B., Meda, P., and Halban, P.A. 1990. Isolation of pancreatic islets and primary culture of the intact microorgans or of dispersed islet cells. *Methods Enzymol.* **192**:188–223.
19. Miki, T., et al. 1998. Defective insulin secretion and enhanced insulin action in K_{ATP} channel-deficient mice. *Proc. Natl. Acad. Sci. USA.* **95**:10402–10406.
20. Parsons, J.A., Bartke, A., and Sorenson, R.L. 1995. Number and size of islets of Langerhans in pregnant, human growth hormone-expressing transgenic, and pituitary dwarf mice: effect of lactogenic hormones. *Endocrinology.* **136**:2013–2021.
21. Gopel, S., Kanno, T., Barg, S., Galvanovskis, J., and Rorsman, P. 1999. Voltage-gated and resting membrane currents recorded from β-cells in intact mouse pancreatic islets. *J. Physiol.* **521**:717–728.
22. Smith, P.A., Ashcroft, F.M., and Rorsman, P. 1990. Simultaneous recordings of glucose dependent electrical activity and ATP-regulated K^+-currents in isolated mouse pancreatic β-cells. *FEBS Lett.* **261**:187–190.
23. Scaglia, L., Cahill, C.J., Finegood, D.T., and Bonner-Weir, S. 1997. Apoptosis participates in the remodeling of the endocrine pancreas in the neonatal rat. *Endocrinology.* **138**:1736–1741.
24. Bonner-Weir, S. 2000. Perspective: postnatal pancreatic β cell growth. *Endocrinology.* **141**:1926–1929.
25. Swenne, I. 1992. Pancreatic β-cell growth and diabetes mellitus. *Diabetologia.* **35**:193–201.
26. Githens, S. 1988. The pancreatic duct cell: proliferative capabilities, specific characteristics, metaplasia, isolation, and culture. *J. Pediatr. Gastroenterol. Nutr.* **7**:486–506.
27. Kaung, H.L. 1994. Growth dynamics of pancreatic islet cell populations during fetal and neonatal development of the rat. *Dev. Dyn.* **200**:163-175.
28. Hugl, S.R., White, M.F., and Rhodes, C.J. 1998. Insulin-like growth factor I (IGF-I)-stimulated pancreatic β-cell growth is glucose-dependent. Synergistic activation of insulin receptor substrate-mediated signal transduction pathways by glucose and IGF-I in INS-1 cells. *J. Biol. Chem.* **273**:17771–17779.
29. Guiot, Y., Henquin, J.C., and Rahier, J. 1994. Effects of glibenclamide on pancreatic β-cell proliferation in vivo. *Eur. J. Pharmacol.* **261**:157–161.
30. Drucker, D.J. 2001. Minireview: the glucagon-like peptides. *Endocrinology.* **142**:521–527.
31. Kim, S.K., and Hebrok, M. 2001. Intercellular signals regulating pancreas development and function. *Genes. Dev.* **15**:111–127.
32. Shiozaki, S., et al. 1999. Impaired differentiation of endocrine and exocrine cells of the pancreas in transgenic mouse expressing the truncated type II activin receptor. *Biochim. Biophys. Acta.* **1450**:1–11.
33. Yamaoka, T., et al. 1998. Hypoplasia of pancreatic islets in transgenic mice expressing activin receptor mutants. *J. Clin. Invest.* **102**:294–301.
34. Kim, S.K., et al. 2000. Activin receptor patterning of foregut organogenesis. *Genes. Dev.* **14**:1866–1871.
35. Mogami, H., et al. 1995. Modulation of adenosine triphosphate-sensitive potassium channel and voltage-dependent calcium channel by activin A in HIT-T15 cells. *Endocrinology.* **136**:2960–2966.
36. Hart, A.W., Baeza, N., Apelqvist, A., and Edlund, H. 2000. Attenuation of FGF signaling in mouse β-cells leads to diabetes. *Nature.* **408**:864–868.
37. Threadgill, D.W., Yee, D., Matin, A., Nadeau, J.H., and Magnuson, T. 1997. Genealogy of the 129 inbred strains: 129/SvJ is a contaminated inbred strain. *Mamm. Genome.* **8**:390–393.
38. Simpson, E.M., et al. 1997. Genetic variation among 129 substrains and its importance for targeted mutagenesis in mice. *Nat. Genet.* **16**:19–27.
39. Ishihara, H., et al. 1995. Inhibition of pancreatic β-cell glucokinase by antisense RNA expression in transgenic mice: mouse strain-dependent alteration of glucose tolerance. *FEBS Lett.* **371**:329–332.
40. Kido, Y., Philippe, N., Schaffer, A.A., and Accili, D. 2000. Genetic modifiers of the insulin resistance phenotype in mice. *Diabetes.* **49**:589–596.
41. Mauvais-Jarvis, F., and Kahn, C.R. 2000. Understanding the pathogenesis and treatment of insulin resistance and type 2 diabetes mellitus: what can we learn from transgenic and knockout mice? *Diabetes Metab.* **26**:433–448.
42. Henquin, J.C., and Meissner, H.P. 1984. Significance of ionic fluxes and changes in membrane potential for stimulus-secretion coupling in pancreatic β-cells. *Experientia.* **40**:1043–1052.
43. Sherman, A. 1996. Contributions of modeling to understanding stimulus-secretion coupling in pancreatic β-cells. *Am. J. Physiol.* **271**:E362–E372.
44. Clocquet, A.R., et al. 2000. Impaired insulin secretion and increased insulin sensitivity in familial maturity-onset diabetes of the young 4 (insulin promoter factor 1 gene). *Diabetes.* **49**:1856–1864.
45. Matsumoto, K., et al. 2000. Increased insulin sensitivity and decreased insulin secretion in offspring of insulin-sensitive type 2 diabetic patients. *Metabolism.* **49**:1219–1223.
46. DeFronzo, R.A., Bonadonna, R.C., and Ferrannini, E. 1992. Pathogenesis of NIDDM. A balanced overview. *Diabetes Care.* **15**:318–368.
47. Kahn, C.R., Vicent, D., and Doria, A. 1996. Genetics of non-insulin-dependent (type-II) diabetes mellitus. *Annu. Rev. Med.* **47**:509–531.
48. Kahn, B.B. 1998. Type 2 diabetes: when insulin secretion fails to compensate for insulin resistance. *Cell.* **92**:593–596.